1954

The effects of magnetic unbalance and mechanical misalignment on the vibration of a D-C motor

Chirillo, Louis D.; Berude, John B.
Massachusetts Institute of Technology

THE EFFECTS OF MAGNETIC UNBALANCE AND MECHANICAL MISALIGNMENT ON THE VIBRATION OF A D-C MOTOR

Louis D. Chirillo

and

John B. Berude

8854
on spine:

CHIRILLO

1954

THESIS
C448

Letter on front cover:

THE EFFECTS OF MAGNETIC UNBALANCE

AND MECHANICAL MISALIGNMENT ON

THE VIBRATION OF A D-C MOTOR

Louis D. Chirillo
and
John B. Berude

THE EFFECTS OF
MAGNETIC UNBALANCE AND MECHANICAL MISALIGNMENT
ON THE
VIBRATION OF A D-C MOTOR

by

LOUIS D. CHIRILLO
Lieutenant, U.S. Navy

B.S., U.S. Merchant Marine Academy
(1950)

JOHN B. BERUDE
Lieutenant, U.S. Navy

S.B., Massachusetts Institute of Technology
(1943)

SUBMITTED IN PARTIAL FULFILLMENT OF THE
REQUIREMENTS FOR THE DEGREE OF
NAVAL ENGINEER

at the

MASSACHUSETTS INSTITUTE OF TECHNOLOGY
(1954)

Massachusetts Institute
of Technology
Cambridge 39, Massachusetts
May 24, 1954

Professor L.F. Hamilton
Secretary of the Faculty
Massachusetts Institute of Technology
Cambridge 39, Massachusetts

Dear Sir:

In accordance with the regulations of the Faculty, we submit herewith a thesis entitled The Effects of Magnetic Unbalance and Mechanical Misalignment on the Vibration of a D-C Motor, in partial fulfillment of the requirements for the degree of Naval Engineer.

Respectfully yours,

Louis D. Chirillo
Lieutenant, U.S. Navy

John B. Berude
Lieutenant, U.S. Navy

THE EFFECTS OF MAGNETIC UNBALANCE AND MECHANICAL MISALIGNMENT ON THE VIBRATION OF A D-C MOTOR

by

LOUIS D. CHIRILLO
Lieutenant, U. S. Navy

and

JOHN B. BERUDE
Lieutenant, U. S. Navy

Submitted to the Department of Naval Architecture and Marine Engineering on May 24, 1954, in partial fulfillment of the requirements for the degree of Naval Engineer.

ABSTRACT

Six parameters may affect the vibration of a direct-current motor:

(a) air-gap eccentricity
(b) motor loading
(c) relative strengths of main field poles
(d) asymmetry of armature construction
(e) dynamic balance of the armature
(f) condition and type of bearings

The object of this thesis was to investigate the effects of air-gap eccentricity on the vibration of a direct-current motor operating at no load and partial load.

Previous attempts to determine the effect of air-gap eccentricity were nullified by end-bell removal, which introduced another variable. In earlier investigations, motor load applied by means of a prony brake introduced vibration frequencies which could not be attributed definitely to the prony brake.

Both difficulties have been overcome in this investigation. Eccentric sleeves fitted in each bearing housing permitted controlled variation of air-gap eccentricity without disturbing the motor end-bells. An integral-mounted eddy-current brake assembly permitted load application without introducing unrecognizable frequencies.

Vibration data were recorded and analyzed for no-load and partial-load motor operation at armature positions varying between centered and 0.0386 inch off-center.

Air-gap flux-density distribution data were recorded using a search loop on the armature surface. These data

were used in predicting the vibration level of the slot-frequency component of total motor vibration.

Conclusions drawn from this investigation are:

(1) Measurement and analysis equipment and technique have a high degree of precision.

(2) Over-all vibration level varies directly with armature displacement.

(3) Slot-frequency vibration level varies directly with armature displacement, and is caused by ~~slot-frequency~~ total flux pulsations under the pole faces.

(4) Correlation between observed and predicted slot-frequency vibration levels is excellent at small armature displacements, but as armature displacement increases, the difference between predicted and observed levels increases.

Recommendations for future study in this field are:

(1) An improved eddy-current brake assembly and air-gap search-loop system should be used to obtain more accurate data under full motor load operation.

(2) Investigations of the effect of unbalanced main field-pole strengths, acting alone and in concert with air-gap eccentricity, should be made.

(3) Armature tooth-slot configuration should be investigated to determine the optimum for vibration reduction purposes.

(4) A phase-sensitive circuit should be used to evaluate the type of motion experienced by the mounted motor to yield information valuable in the design of resilient motor mountings.

Any improvement in the concentricity of armature and pole surfaces will reduce the vibration level of an existing motor if adjustment of poles is achieved with the use of high-permeability shim stock.

Thesis Supervisor: D. C. White
Title: Assistant Professor of Electrical Engineering

ACKNOWLEDGMENTS

The authors are indebted to Professor D.C. White, of the Electrical Engineering Department, Massachusetts Institute of Technology, for his advice and guidance; to Commander W.H. Simpson, U.S. Navy, attached to the Boston Naval Shipyard, for making available the equipment used; and to other personnel attached to the Design Division of the Planning Department, Boston Naval Shipyard, for advice, instruction, and assistance in its operation; to Mrs. Bertha Hornby for her patience, forbearance, and skill in preparing the thesis in its final form; and to the large number of people at the Massachusetts Institute of Technology and the Boston Naval Shipyard who helped make this project an enjoyable as well as an educative experience.

TABLE OF CONTENTS

	Page
ABSTRACT	ii
ACKNOWLEDGMENT	iv
I. INTRODUCTION	1
II. PROCEDURE	5
Preparation of Equipment	5
Data Recording Procedure	7
Analysis Procedure	9
Calculations	10
III. RESULTS	22
IV. DISCUSSION OF RESULTS	26
No-Load Condition	26
Partial-Load Condition	28
V. CONCLUSIONS	32
VI. RECOMMENDATIONS	33
APPENDIX A. CALCULATIONS	35
APPENDIX B. DATA	42
APPENDIX C. MOTOR IDENTIFICATION	48
APPENDIX D. LITERATURE CITATIONS	49

I

INTRODUCTION

For various tactical and defensive reasons, the noise output of submarine machinery must be reduced. Some of the machinery that must be operated during "noise" critical periods are driven by direct-current motors.

Pitched noises, such as those made up of definite frequency components related to the rotating speed of an electric motor, are more susceptible to recognition in an undersea ambient than are random noises. One remedial measure is to employ resilient mountings, which permit a motor to vibrate while attenuating to some degree the forces transmitted to the sea via the motor foundation and the submarine hull structure. The objectives of recent programs of study have been to reduce the generation of noise at its source.

In the previous studies of electrical rotating machinery, certain predominant frequencies have exhibited themselves. In order to effect any significant noise reduction, it is necessary that the predominant frequencies be reduced. The reduction in level or even elimination of a subordinate frequency component will be of no significance. This is due to the fact that the levels are logarithmic functions of a ratio of voltages

(output of vibration pickup/reference voltage) expressed in decibels. Consider, for example, two components: one of 100 decibels level, and the other of 90 decibels. Their combined level is only 100.42 decibels. Accordingly, elimination of the 90 decibels component still leaves the 100-decibel component; the reduction is an insignificant 0.42 decibel.

Some of the predominant frequency components of electrical rotating machinery have been identified as being definite functions of certain operational characteristics of the machine. A systematic procedure, conducted at the Boston Naval Shipyard, for effecting unbalance of a rotor caused a definite increase in level of the frequency corresponding to the first order of the operating speed. In another investigation, personnel of the Boston Naval Shipyard have established that the frequency corresponding to the third order of the operating speed was attributed to a specific type of ball bearing commonly used in submarine machinery.

One predominant peak appearing in the frequency spectrum of a direct-current electric motor is the product of the number of rotor slots and the rotational speed; it is termed "slot frequency." The fact that this frequency component is a function of the air-gap resultant flux-density distribution is evidenced by its absence when a rotor is driven in the absence of a magnetic field, as in

a dynamic balancing process. In view of this, it is probable that the slot-frequency vibration is incurred by force fluctuations which are a result of the periodic variation in radial reluctance paths as the armature slots pass beneath the pole faces. This view is supported by Wiesemann,[15] who specifically states that if the number of armature teeth spanned by a pole varies when the pole is moved through a tooth pitch, the flux will pulsate.

It is the purpose of this thesis to evaluate the effect on vibration of magnetic-field anomalies which would amplify the flux pulsations mentioned by Wieseman[15] so as to increase the noise level of the slot-frequency component. These magnetic-field anomalies may result from eccentricity of air gap, unbalance of field-pole strengths, or asymmetry of armature construction.

Based on the experiences of a special submarine machinery repair facility at the Boston Naval Shipyard, it was learned that the over-all vibration output of a motor would change as much as 5 decibels as a result of merely loosening and retightening the end-bells. Even though the end-bells were carefully secured with torque wrenches, this variation persisted. Therefore it was necessary to devise means for effecting eccentricity of air gap and unbalance of field-pole strength without resorting to removal of the end-bells so as to obtain good repeatability of data. The effects of asymmetrical

a typical balancing process. In view of this, it is probable that the slot-frequency vibration is imported by force fluctuations which are a result of the periodic variation in radial reluctance paths as the armature slots move beneath the pole faces. This view is supported by Alexander,[12] who specifically stated that if the number of armature teeth spanned by a pole varies when the pole is moved through a tooth pitch, the flux will pulsate.

It is the purpose of this thesis to evaluate the effect on vibration of magnetic-field anomalies which would amplify the flux pulsations mentioned by Alexander[12] so as to increase the noise level of the slot-frequency component. These magnetic-field anomalies may result from eccentricity of the gap, unbalance of field-pole strengths, or asymmetry of armature construction.

Based on the experiences of a special submarine auxiliary repair facility at the Boston Naval Shipyard, it was learned that the slot-frequency vibration output of a motor would change as much as 5 decibels as a result of merely loosening and retightening the end-bells. Even though the end-bells were carefully assembled with feeler gauges, this variation persisted. Therefore it was necessary to devise means for effecting eccentricity of the gap and unbalance of field-pole strengths without resorting to removal of the end-bells so as to assure good repeatability of data. The effects of asymmetrical

armature construction and unbalanced main field-pole strengths were not investigated.

II

PROCEDURE

PREPARATION OF EQUIPMENT

The entire motor (and eddy-current brake assembly for the loaded motor condition) was mounted on rubber-bonded springs which were, in turn, supported by a heavy structural steel table. The assembly had a natural frequency of about four cycles per second. A low natural frequency was desired so that resonance effects caused by the mounting system would be negligible at frequencies near and exceeding the frequency corresponding to motor rotative speed. Figure I illustrates the mounting arrangement, and also shows the eddy-current brake assembly and mounted vibration pickups.

An eddy-current brake was modified by evenly spacing three magnetic coils, rather than the usual two, around the aluminum disk. A special foundation and shaft support for the brake was made so that the complete brake assembly could be mounted directly on the foundation supporting the motor. In this manner a monolithic structure was assembled, all parts being subjected to the same disturbing forces and supported by a common foundation. The eddy-current brake was a part of the over-all structure only during the load tests. During the no-load tests it was not attached in any way to the motor assembly. The use of an eddy-current brake

eliminated unpredictable and unrecognizable vibrations such as would result if a prony brake were used.

The motor armature was dynamically balanced to within 11 micro-inches displacement at maximum operating speed using a Gisholt balancing machine.

Main field poles and interpoles were removed, cleaned, and adjusted to obtain reasonably accurate concentricity between the armature and the motor poles. After adjustment, using transformer-steel shim stock, the actual air gap differed from the designed air gap by a maximum of 0.0023 inch, and the average corrected air gap was measured to be 0.0002 inch greater than the designed air gap of 0.0625 inch. Before adjustment, the corresponding figures were 0.010 inch maximum difference and 0.007 inch average difference. The latter measurements represent part of the results of a standard noise-reduction program, and are less than the figures for the motor as received from the manufacturer. Figures II, III, and IV illustrate the techniques followed and equipment used in adjusting the air gaps.

Eccentric location of the armature with respect to the motor poles was made possible by fitting calibrated dual eccentric sleeves between each bearing and its housing. The eccentric sleeves were calibrated in ten-degree intervals. With this arrangement the armature could be moved linearly in any direction without removing the end-bells. The important influence of end-bell manipulation on over-all

noise level was thereby eliminated at its source. Figures V and VI show the arrangement and dimensions of the eccentric sleeves, and show the relationship between the angular rotation of the sleeves and resultant linear translation of the armature.

To permit controlled variation of the motor pole strengths, external connections were provided to both field and armature circuits. Throughout the tests, balanced field strengths were maintained.

A thin wire voltage pickup was glued to the surface of the armature and connected to copper slip rings on the motor shaft. The induced voltage was impressed on a voltage calibrated oscilloscope, and the air-gap flux-density waveform was recorded on film with a Polaroid-Land Camera. Figure VII shows the air-gap search-coil assembly.

DATA RECORDING PROCEDURE

Vibration data were obtained for no-load and partial-load (1.2 horsepower) conditions with the armature in different positions. For both load and no-load conditions, data were recorded for the following armature positions: centered, and offset 0.0104, 0.0205, 0.0300, 0.0386 inch toward a main field pole. During the no-load tests the motor speed was 2100 RPM (35 CPS), and during the load tests it was 2000 RPM (33.3 CPS).

Figure VIII illustrates the recording equipment used and its arrangement.

The Massa Accelerometer is an inertia-operated crystal pickup which generates a voltage (later amplified by the Massa Preamplifier) proportional to the acceleration of the vibrating body. Calibration of the pickup recording system yielded the information that the system frequency limitations lie between 20 CPS and 8000 CPS. This frequency limitation includes the effects of the pickup, its preamplifier, the Magnecorder Amplifier and Recorder, and the magnetic recording tape, which was commercial Audiotape having a copper-oxide base. The Magnecorder Amplifier Model PT63AH-Recorder Model PTZ-P system has a flat frequency characteristic between 20 and 10,000 CPS. The recorded data represent peak accelerations expressed in decibels. Peak velocity or displacement at a specific frequency may be calculated by dividing peak acceleration by the frequency or by the frequency squared, respectively.

Vibration data were initially recorded with the pickup located at diagonally opposite feet of the motor, and on each foot, at each of three mutually perpendicular axes. The three axes were: (1) horizontal and parallel to the motor shaft, (2) horizontal and perpendicular to the motor shaft, and (3) vertical and perpendicular to the motor shaft. Analysis of these data indicated that, for the frequency range of interest, no significant variations existed between the data recorded with different pickup positions. In subsequent runs the data were therefore taken with the pickup

in the vertical position only. Duplicate sets of data were recorded for each armature position during the no-load test to determine the precision (repeatability) of measurements. The data obtained with the fixed pickup position (See Tables I and II, Appendix B) were used as the basis for vibratory force calculations.

The voltage induced in the wire pickup by the air-gap flux was recorded for all armature positions during the no-load tests only. Since the maximum load obtainable (1.2 horsepower) was only 20 per cent of the rated motor load, it was considered that there would be no significant differences in air-gap flux density between the no-load and load motor conditions.

Load was applied to the motor by means of the eddy-current brake. Current through the brake coils was monitored, and was controlled by large resistors connected in series with the brake coils.

ANALYSIS PROCEDURE

Figure IX shows the equipment used in the analysis procedure.

The General Radio Type 760-A Sound Analyzer is a continuous-spectrum frequency-selective instrument having a degenerative feedback characteristic at all frequencies except that to which it is tuned. It is a sensitive, narrow-band filtering device ideally suited to the analysis of the types of pitched noise (vibration) encountered in this project.

The Sound Apparatus Company Graphic Level Recorder Type FR, when used in conjunction with the Sound Analyzer, records a curve of amplitude versus frequency of the vibrating object. With this system, synchronism between the motion of the paper in the recorder and the Sound Analyzer frequency sweep rate is maintained by a chain connection between the two instruments.

The Oscillator-Calivolter system is used to impress on the graphic record a calibrated noise level, so that the magnitude of the noise level at any particular frequency may be determined. The Calivolter is merely a potentiometer-type instrument which can be adjusted to give a constant voltage output.

Using this system, noise levels were determined graphically for important discrete frequencies. The important frequencies are the fundamentals and harmonics of motor rotative and armature slot frequencies. The over-all accuracy of the recording and analyzing methods used is considered to be ± 2 decibels. The noise levels at the critical frequencies were plotted to show the variation of vibration with armature position.

CALCULATIONS

From the recorded acceleration data expressed in decibels, actual vibratory accelerations corresponding to slot frequency in the no-load test were calculated, using the

calibrated sensitivity of the accelerometer pickup system. From the accelerations, and using the known mass of the motor system, the actual vibratory forces acting on the motor foundation were calculated.

These vibratory forces were compared with those calculated using a theoretical approximate approach as follows:

(1) The peak air-gap flux density for each armature position of the no-load test was calculated using the equation

$$e = B \times \ell \times v \tag{1}$$

in which e = the electromotive force induced in the wire pickup located on an armature tooth, volts

B = air-gap flux density, lines/cm^2

ℓ = wire pickup length, cm

v = rate at which flux lines were cut by the wire pickup, cm/sec

(2) Based on Wieseman's results,[15] the flux-density pulsation under each main field pole was calculated. The instantaneous flux-density distribution was assumed to be sinusoidal.

(3) The instantaneous flux-density distribution was integrated across each pole face to obtain the total flux under the pole.

(4) The instantaneous attractive force between the armature and each pole face was calculated using the equation

$$f = \frac{1}{2}\frac{\phi^2}{\mu A} \tag{2}$$

in which f = attractive force between armature and pole, newtons

ϕ = total flux under a pole face, webers

μ = air-gap permeability = $4\pi \times 10^{-7}$ weber/amp-turn-meter

A = area of each pole face, meter^2

(5) A scaled layout of a segment of the armature surface and a complete pole face was made. The relative angular position of pole faces and armature was adjusted to determine the orientation yielding the maximum total vector attractive force between all pole faces and the armature. For this angular position, and for each lateral armature position, the attractive force between each pole and the armature was calculated as described above.

(6) These forces for the individual poles were combined to give the magnitude and direction of the total resultant vibratory force acting on the motor foundation. The vertical component of this force was compared with that obtained directly from recorded data.

FIG. I

MOTOR MOUNTING ARRANGEMENT

NO-LOAD TEST

LOAD TEST WITH EDDY-CURRENT BRAKE

FIG. II

POLE ADJUSTMENT TECHNIQUE

FIG. III

POLE ADJUSTING TECHNIQUE

CLOSE UP

FIG. IV

POLE ADJUSTING TECHNIQUE

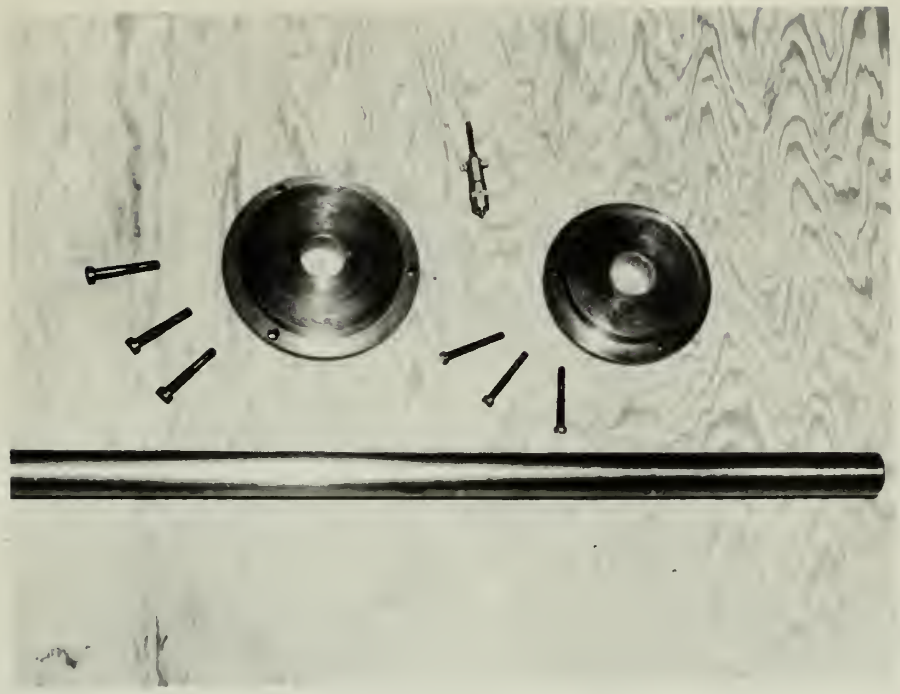

END PLUGS AND MANDREL

FIG. V

ECCENTRIC SLEEVE ASSEMBLY AND DETAILS

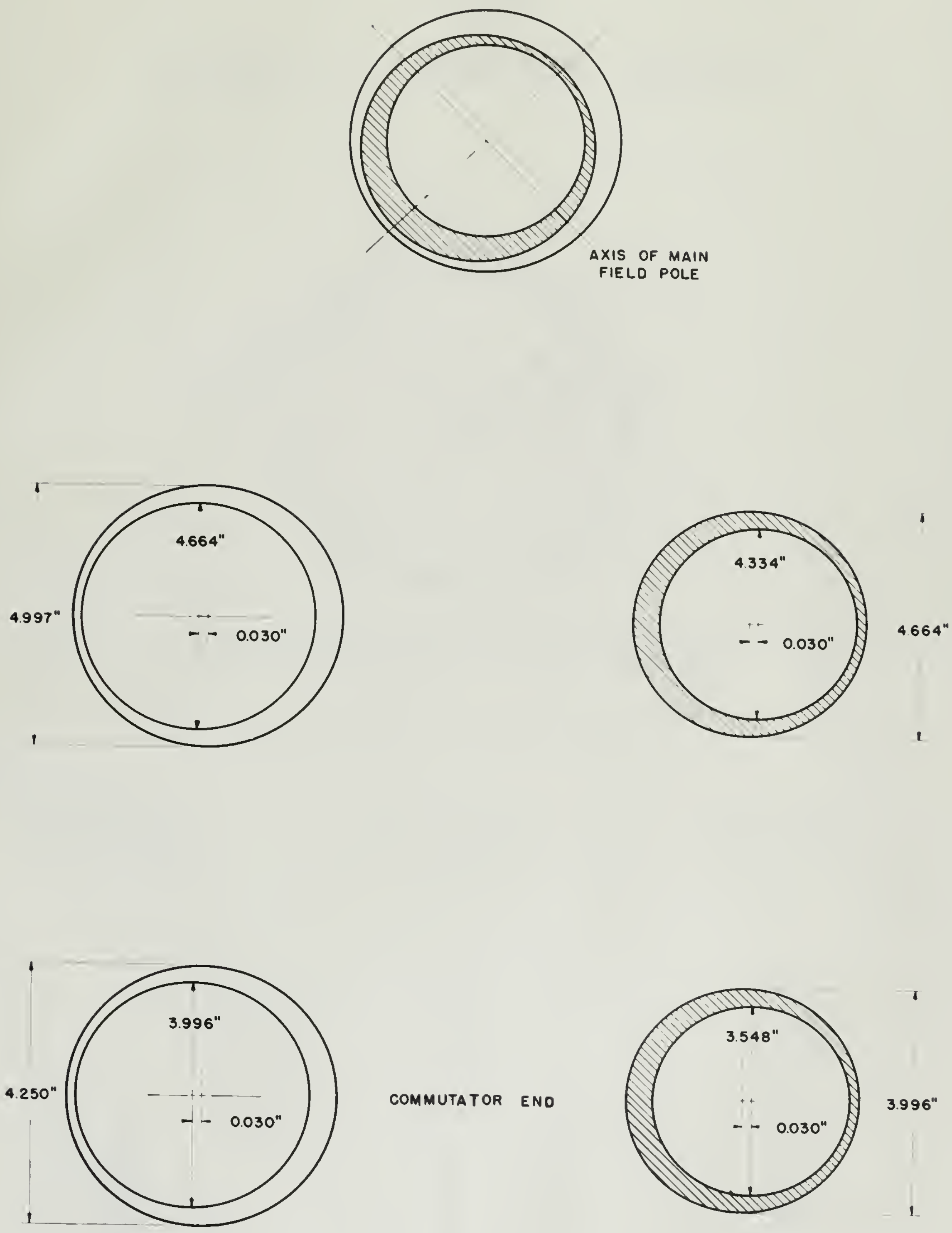

FIG. VI

LOCUS OF ARMATURE CENTER

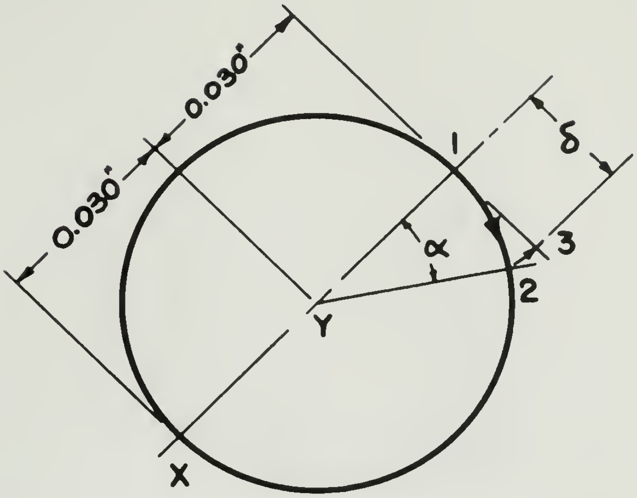

$$\delta \text{ (MILLS)} = 2 \times 30 \sin\left(\frac{\alpha}{2}\right)$$

Path of Center: 1 ⟶ 2 ⟶ 3

Ang. Rotation of Inner Sleeve deg. (clockwise)	Ang. Rotation of Outer Sleeve deg. (counter-clock.)	Displacement from True Center (Pt. 1) mills
0	0	0
10	5	5.2
20	10	10.4
30	15	15.5
40	20	20.5
45	22.5	23.0
50	25	25.4
60	30	30.0
80	40	38.6
100	50	46.0
120	60	52.0
140	70	56.3
160	80	59.1
180	90	60.0

FIG. VII

AIR GAP SEARCH LOOP

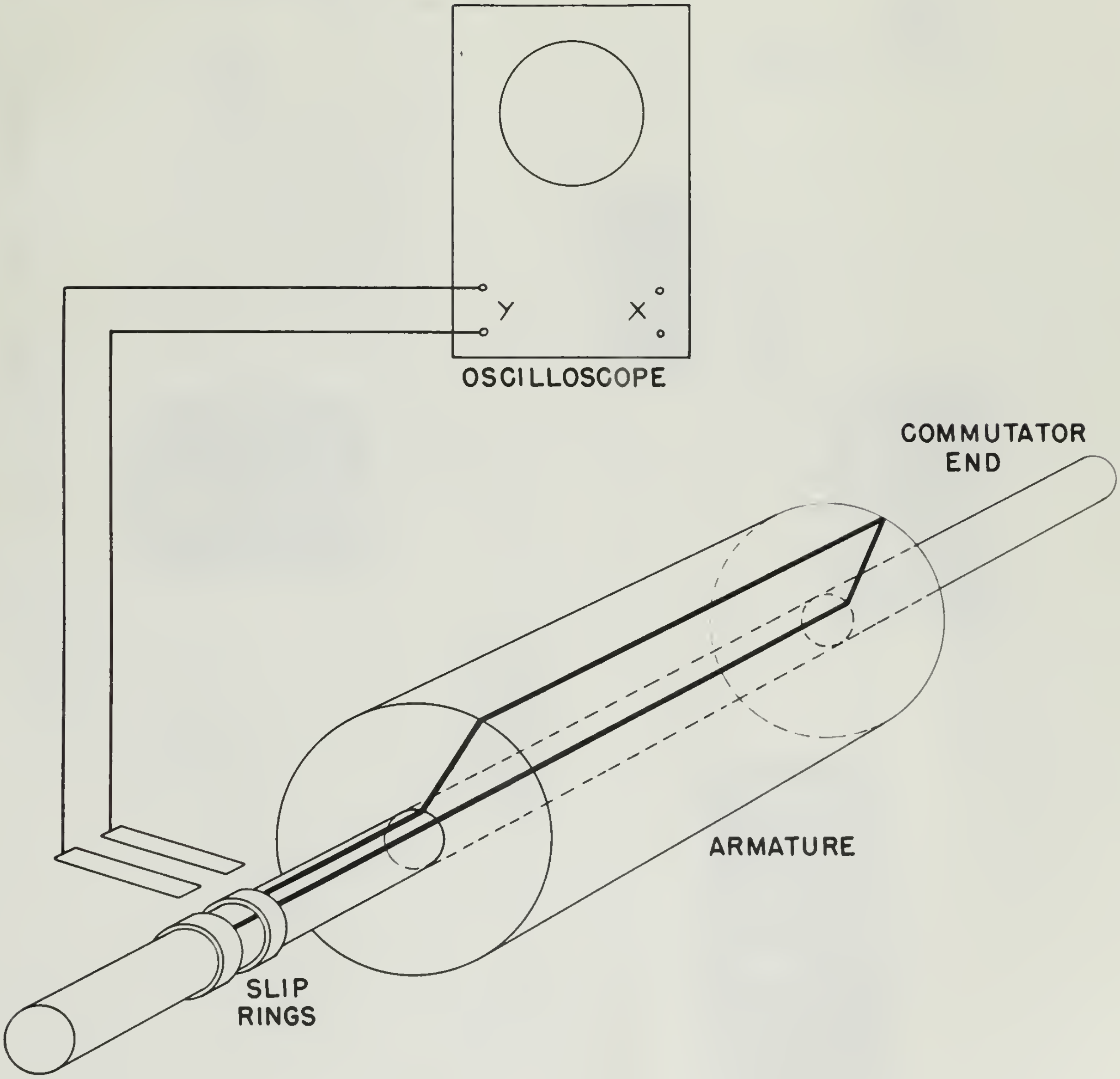

FIG. VIII

VIBRATION RECORDING INSTRUMENTATION

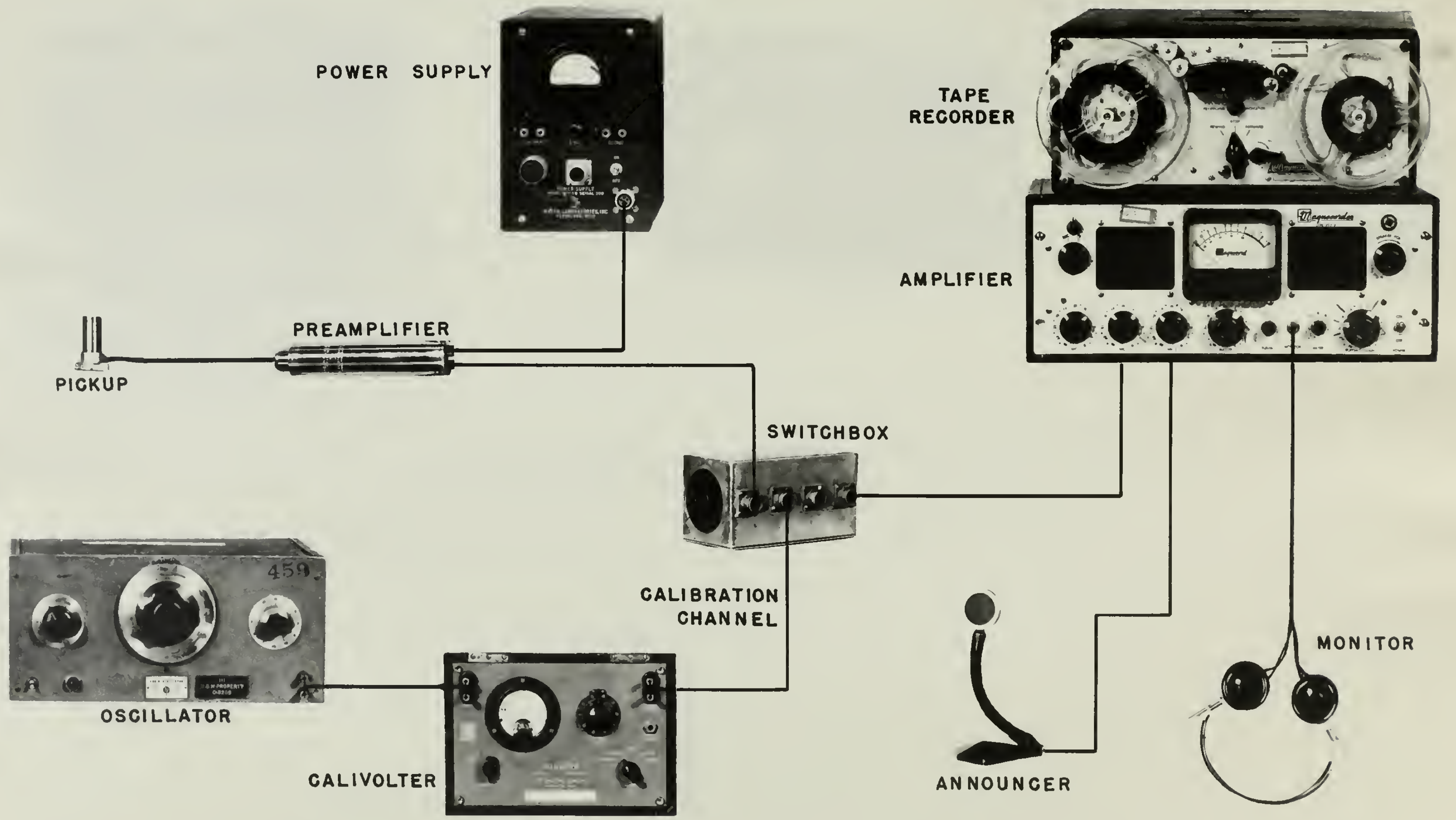

FIG. IX

VIBRATION ANALYZING INSTRUMENTATION

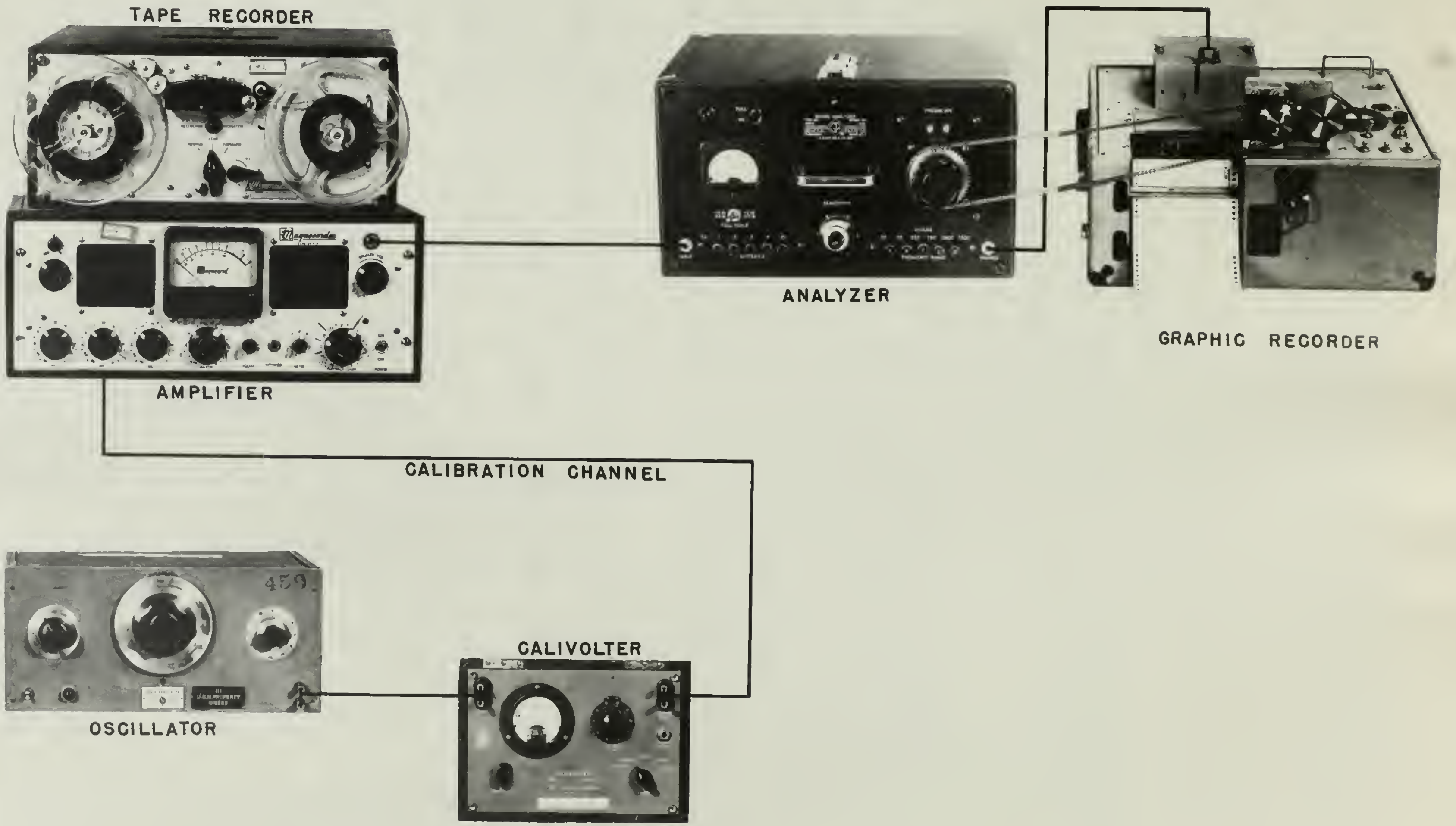

III

RESULTS

The results of this investigation are shown in Tables I, II, and III, and in Figures X, XI, and XII.

Tables I and II permit conclusions to be drawn regarding the precision of the method of recording and analyzing data in the no-load series of tests.

Figure X shows the effect of air-gap eccentricity (armature displacement) on the over-all vibration level and on the contributions of important discrete operating frequencies of the motor under no-load conditions. Figure XII gives the same information for partial-load motor operation.

Figure XI offers a comparison between predicted and observed vibration levels at slot frequency for the no-load operating condition.

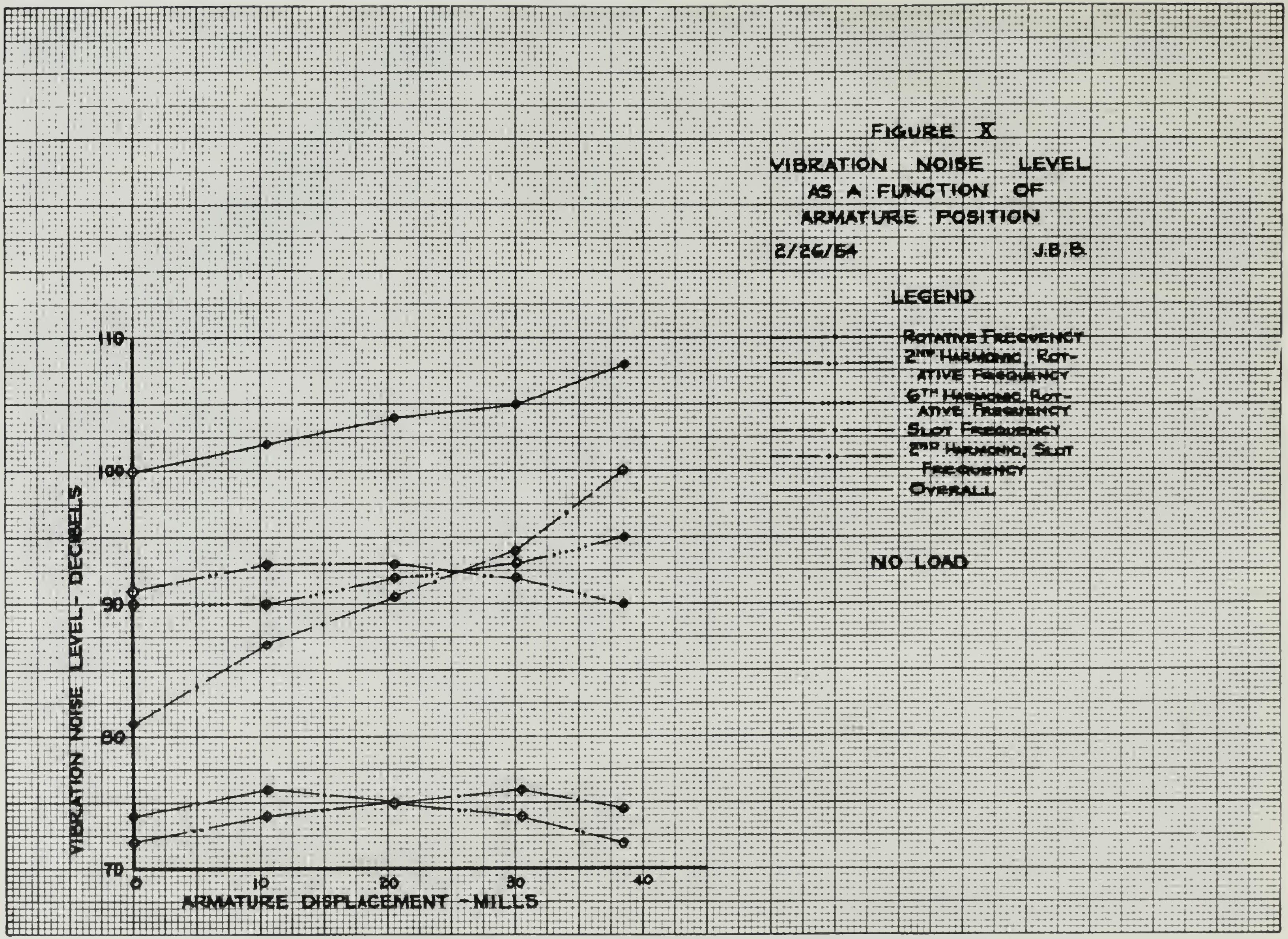
FIGURE X
VIBRATION NOISE LEVEL AS A FUNCTION OF ARMATURE POSITION
2/26/54
J.B.B.
LEGEND
ROTATIVE FREQUENCY
2ND HARMONIC, ROTATIVE FREQUENCY
6TH HARMONIC, ROTATIVE FREQUENCY
SLOT FREQUENCY
2ND HARMONIC, SLOT FREQUENCY
OVERALL
NO LOAD
VIBRATION NOISE LEVEL - DECIBELS
110
100
90
80
70
0
10
20
30
40
ARMATURE DISPLACEMENT - MILLS

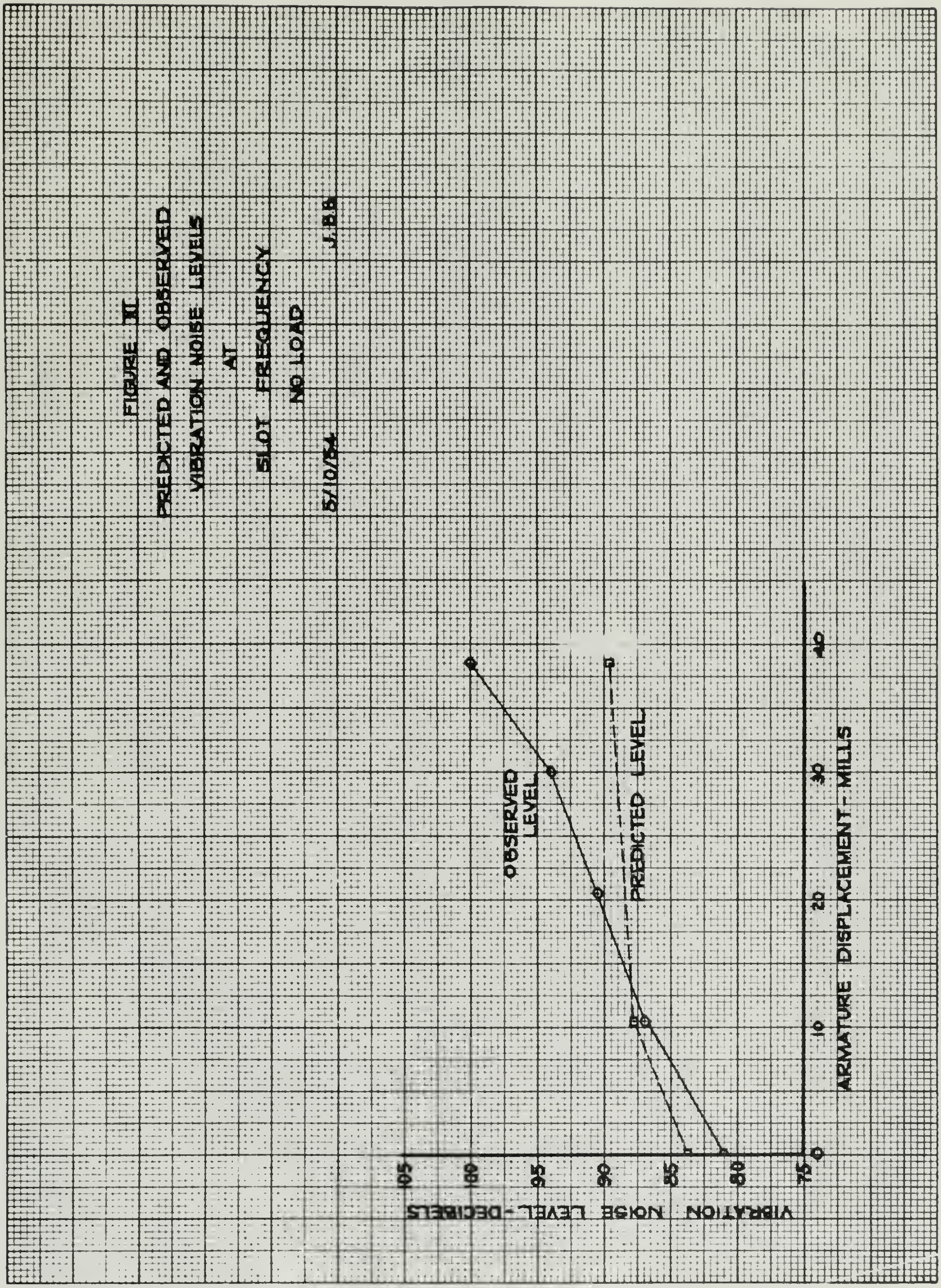
FIGURE XI
PREDICTED AND OBSERVED
VIBRATION NOISE LEVELS
AT
SLOT FREQUENCY
NO LOAD
5/10/54
J.B.B.
OBSERVED LEVEL
PREDICTED LEVEL
ARMATURE DISPLACEMENT - MILLS
0
10
20
30
40
VIBRATION NOISE LEVEL - DECIBELS
75
80
85
90
95
100
105

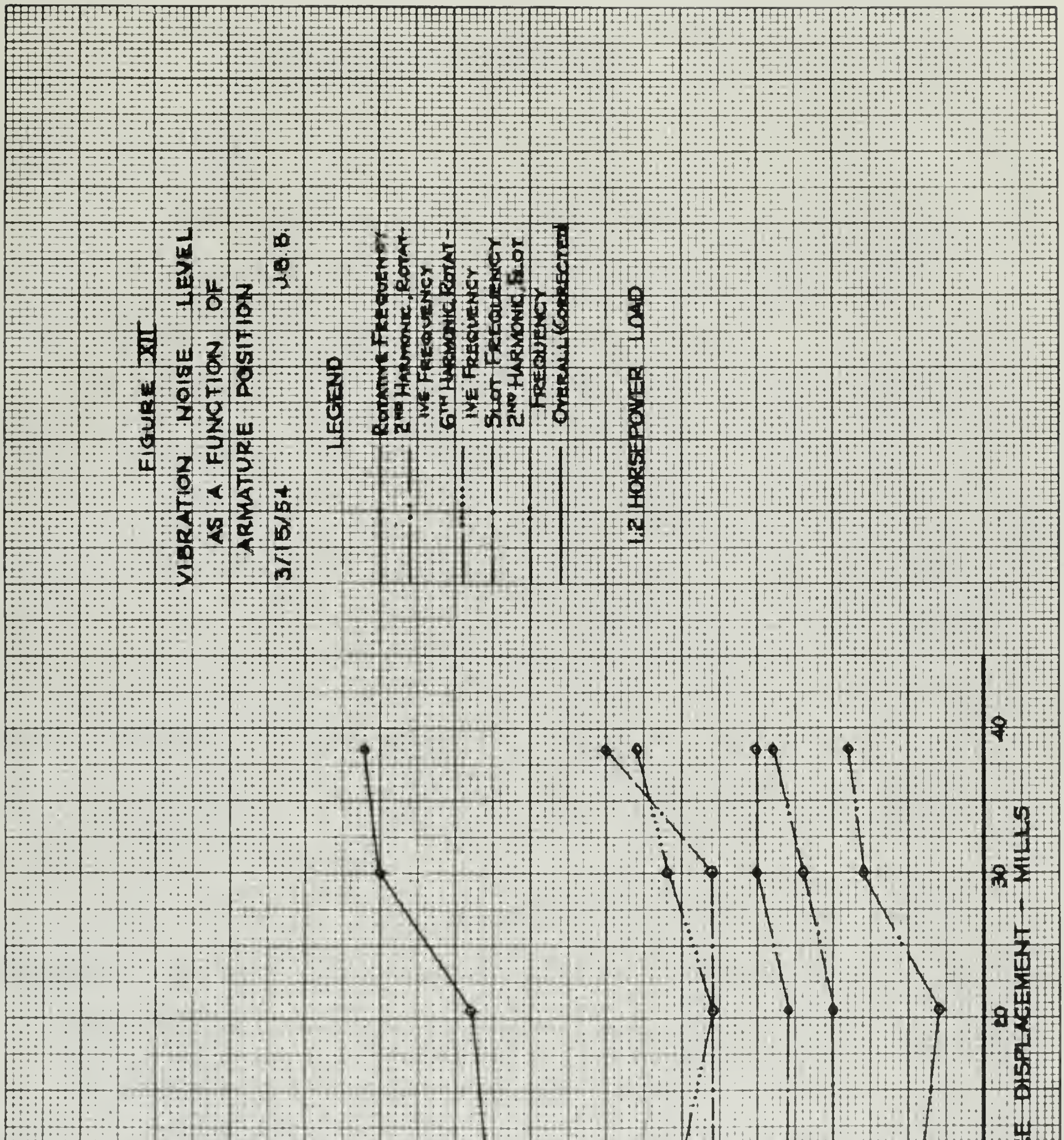

FIGURE XII
VIBRATION NOISE LEVEL
AS A FUNCTION OF
ARMATURE POSITION
3/15/54 J.B.B.
LEGEND
ROTATIVE FREQUENCY
2ND HARMONIC, ROTATIVE FREQUENCY
6TH HARMONIC ROTATIVE FREQUENCY
SLOT FREQUENCY
2ND HARMONIC SLOT FREQUENCY
OVERALL (CORRECTED)
1.2 HORSEPOWER LOAD
VIBRATION NOISE LEVEL - DECIBELS
120
110
100
90
80
0
10
20
30
40
ARMATURE DISPLACEMENT - MILLS

IV

DISCUSSION OF RESULTS

NO-LOAD CONDITION

The results of the no-load vibration data and calculations for a balanced-rotor direct-current motor with balanced main field-pole strengths show that:

(1) The degree of precision (repeatability) of vibration data measurements and analysis is ± 2 decibels.

(2) The over-all vibration level increases almost linearly with armature displacement from the true centered position. The rate of increase is approximately one decibel per 0.005 inch of armature displacement: that is, the vertical component of the vibrating force transmitted to the motor foundation is doubled for each 0.030-inch increment of armature displacement.

(3) For armature displacements less than about 0.025 inch, two specific frequencies dominate: sixth-harmonic of the motor rotative frequency, and second-harmonic of the slot frequency. For larger armature displacements, slot frequency predominates. Though other discrete frequencies contribute to the over-all vibration level, they are of lesser importance.

(4) The "base" vibration level is established by the sixth-harmonic of motor rotative frequency and by the second-harmonic of slot frequency. The variation of vibration level with armature displacement is established by the

slot-frequency vibration level. The slot-frequency vibration level increases almost linearly with armature displacement, the rate of increase being approximately one decibel per 0.002 inch of armature displacement: that is, the component of vibration caused by slot frequency doubles for each 0.012-inch increment of armature displacement.

(5) Calculations (Appendix A) show that the total flux under a main field pole varies cyclically, with a frequency identical with slot frequency. Vibratory forces caused by the flux variation were also shown to occur at slot frequency.

(6) For small armature displacements, close agreement exists between observed vibration levels at slot frequency and those predicted on the basis of an assumed sinusoidal air-gap flux-density distribution under each pole face. For a large armature displacement, the predicted slot-frequency vibration level was only about two-thirds the observed. As armature displacement increases beyond approximately one-third the designed air gap, the observed slot-frequency vibration level becomes increasingly greater than the predicted level.

As the armature is moved toward a main field pole, the mean flux density under that pole increases to the point where the fluctuations become relatively unimportant. In other words, at large armature displacements the large mean flux density in the reduced air gap is of primary importance, whereas at small armature displacements the sinusoidal flux-density distribution is dominant.

An additional air-gap search loop was located on a pole face in this investigation, but successful operation of this loop was not achieved. Had it been, a record of the actual flux-density pulsations faced by the main field poles would have been obtained. The necessity for assuming a magnitude of flux-density pulsation would have been obviated then, and a more accurate calculation of forces might have been made. If subsequent work is done on this project, the use of an improved pole-face search-loop circuit in conjunction with the already successful one located on an armature tooth should produce more accurate correlation between observed and predicted vibration levels.

PARTIAL-LOAD CONDITION

For partial-load operation of the motor with balanced main field-pole strengths and a balanced rotor:

(1) All vibration levels increased as compared with no-load operation.

(2) The increase of the over-all vibration level with armature displacement was approximately the same as for no-load operation.

(3) Slot frequency and the sixth-harmonic of motor rotative frequency were the most important contributors to the over-all vibration level of the motor.

A maximum load limit of about 16 per cent rated load was imposed by limitations of the eddy-current brake assembly. The aluminum disk was warped to such an extent that fairly

large air gaps had to be maintained between the disk and the magnetic loading coils to avoid contact between them. Also, since soft iron was not available for the magnetic loading coils, steel had to be used, with a resultant increase in reluctance of the magnetic circuits of the eddy-current brake.

In future work, a stiffer eddy-current brake disk should be used. It may be shaped like a steam-turbine disk: that is, thick at the hub and tapered toward the rim. Soft iron should be used in the eddy-current-brake magnetic circuits to make full motor loading possible.

Over-all and slot-frequency vibration levels for both no-load and partial-load operation of the motor vary directly with effective armature displacement from the true motor center. Effective armature displacement may arise in practice in two ways:

(a) by actual translation of the armature from the true motor center. Production-line direct-current motors of similar size are received frequently with armatures displaced by as much as 0.020 to 0.030 inch.

(b) by insertion of brass shim stock under the pole shoes in an attempt to obtain better concentricity between the armature and pole faces. Brass shim stock, because of its relatively low permeability, acts to increase the effective air gap wherever it is used. The effect is identical with that of displacing the armature away from a pole face.

The use of brass shims for this purpose is not uncommon.

When noise is critical, vibration-free motor operation is mandatory. Air-gap eccentricity must be reduced, then, to a practicable minimum determined by a balancing of economic and vibration factors. Transformer steel or soft-iron shim stock, not brass, should be used to obtain the desired degree of concentricity.

Unbalanced main field-pole strengths may have an effect on the level of motor vibration. Interacting or joint effects of unbalanced main field-pole strengths and air-gap eccentricity may also exist. These subjects must be investigated before the problem of vibration of motors can be solved.

The instrumentation used in this investigation could not, because of its nature, yield information on the type of motion produced by the vibrations. The motion of the motor may be translation, rotation, or some combination of the two. Accurate information regarding the type of motion is essential if the motor mounting is effectively to attenuate the vibrations transmitted through the motor frame to its foundation.

A circuit which may be used to obtain this information is shown in Figure XIII. This system involves the use of two accelerometer pickups, a Z-axis oscilloscope and a "circular sweep circuit" developed by K. Lee, of the Planning Department, Boston Naval Shipyard. With this system, the magnitudes and phase relation between two acceleration vectors can be determined, from which the type of motion may be deduced.

FIG. XIII

RECOMMENDED CIRCUIT FOR MEASURING MAGNITUDE AND PHASE OF VIBRATION

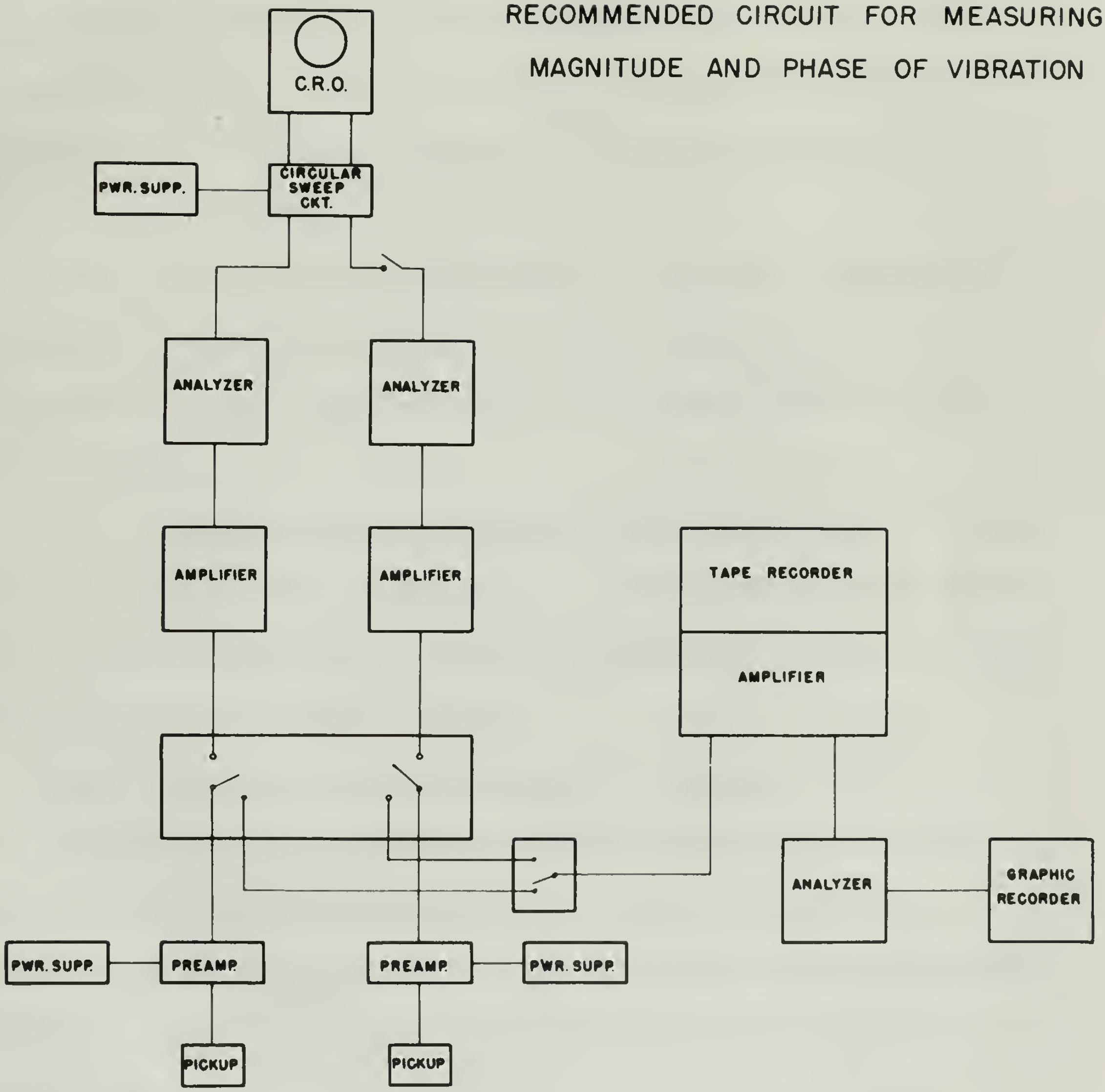

V

CONCLUSIONS

Conclusions which may be drawn from this investigation are:

(1) The vibration measuring and analysis system used was accurate and had a high degree of precision.

(2) Over-all vibration level varies directly with armature displacement, doubling for each 0.030-inch increment of armature displacement.

(3) Slot-frequency vibration is a major component of over-all vibration level, and is the frequency causing variation of the over-all vibration level with armature displacement.

(4) Slot-frequency vibration is produced by periodic air-gap flux-density pulsations. The period of each pulsation is identical with that of a single slot-tooth combination rotating at motor speed.

(5) Excellent correlation existed between observed and predicted slot-frequency vibration levels at small armature displacements and under no-load operation. At a large armature displacement, the predicted slot-frequency vibration level was approximately 70 per cent of the observed level.

VI

RECOMMENDATIONS

Recommendations for future work in the field of this investigation are:

(1) Obtain vibration data at rated motor load by improving the eddy-current brake assembly. Improvements should include a disk shaped to obtain greater stiffness, and the use of soft-iron cores in the eddy-current-brake magnetic circuits.

(2) An air-gap search loop located on the surface of a main field pole should be employed in conjunction with one located on an armature tooth when vibration data are measured. Accurate information on the amplitude of flux-density pulsation under the pole face may be obtained in this manner, and more accurate predictions of the slot-frequency vibration level may be made.

(3) Investigations should be made to determine the effect on the motor vibration level of unbalanced main field-pole strengths acting alone, and acting together with air-gap eccentricity.

(4) To evaluate the type of motion produced by the vibrations, the circuit shown in Figure XIII may be used. Information on the motion is necessary if efficient vibration attenuating mountings are to be developed.

(5) A study should be made of armature tooth-slot

configurations in order to evolve a design which will minimize flux-density pulsations.

Recommendations as to methods of reducing the vibration generated in direct-current motors are:

(a) Adjust the motor poles to obtain a practicable degree of concentricity between the armature and pole-face surfaces.

(b) Adjustment of poles should be made with soft-iron or transformer-steel shim stock, not the usual brass.

APPENDIX A

APPENDIX A

CALCULATIONS

Assumption: Sinusoidal distribution of flux density between the armature and the pole faces:

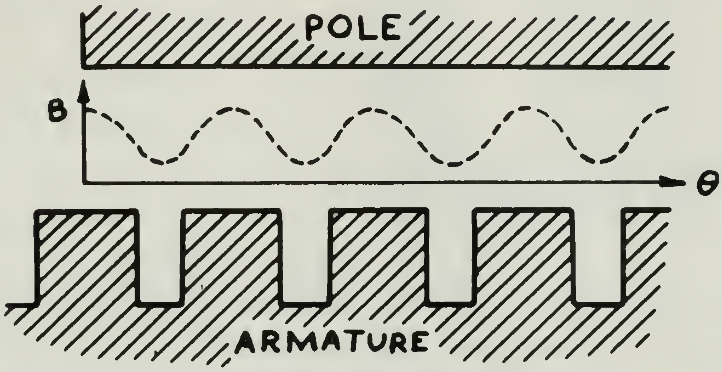

Approximations: The pole widths were measured to the nearest degree in order to more easily facilitate the evaluation of trigonometric functions:

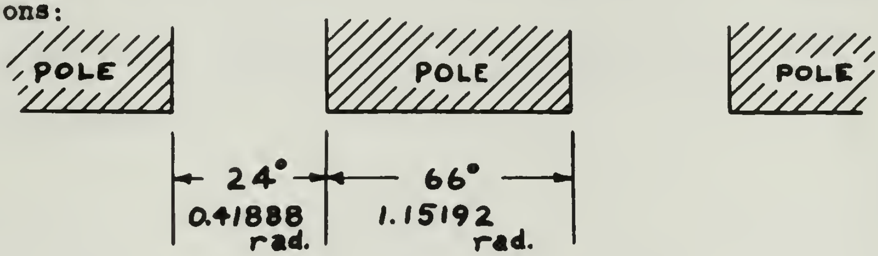

Armature Geometry:

Diameter = 8.01 inches

Circumference = 25.164 inches

Number of slots = 37

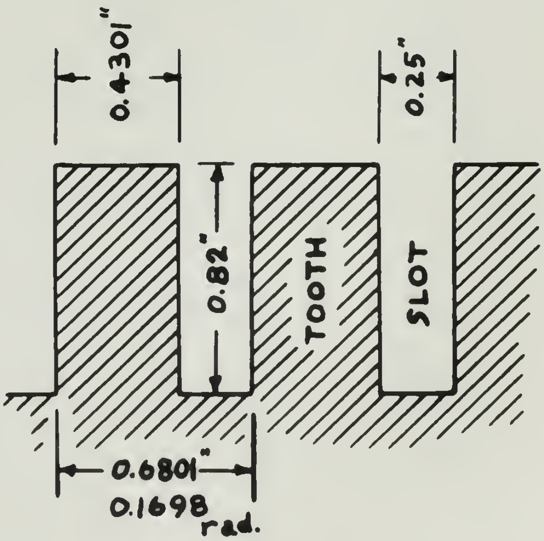

Function Describing Flux-Density Distribution: The air-gap search loop was installed on the center of an armature tooth. In that the tooth region comprises a low reluctance path as compared to the slot region, the voltage induced in the air-gap search loop is proportional to the maximum flux density, B_{max}:

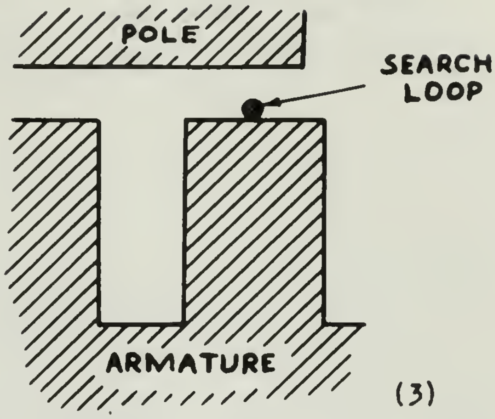

$$B_{max} = \frac{e}{l\ v} \tag{3}$$

where e is the electromotive force induced in the loop,
l is the effective length of the loop (equivalent to the axial pole length), and where
v is the peripheral speed of the loop.

The flux-density pulsation coefficient, k, was obtained in each case for a given slot width/air gap ratio from a plot prepared by Wieseman(15). The product $k\ B_{max}$ is the magnitude of the flux-density pulsation:

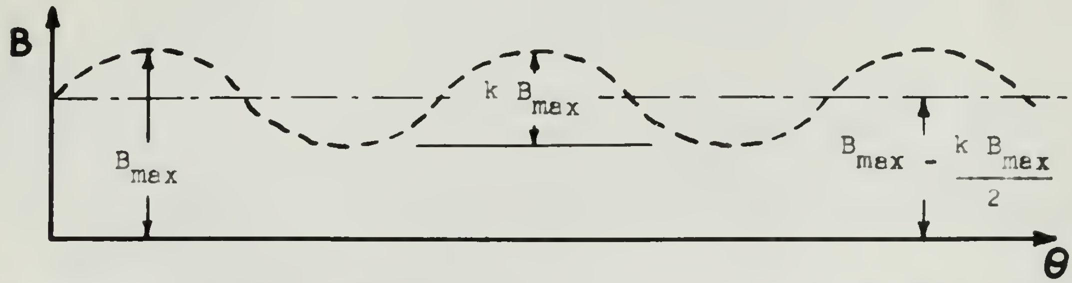

Accordingly the flux-density distribution in the air gap as a function of angular displacement, θ, is:

$$B = B_{max} - \frac{k\ B_{max}}{2} + \frac{k\ B_{max}}{2} \cos 37\theta \tag{4}$$

or:

$$B = B_{max}\left(1 - \frac{k}{2} + \frac{k}{2} \cos 37\theta \right) \tag{5}$$

Total Flux per Pole: An element of area per incremental angular displacement, $d\theta$, is $l\ r\ d\theta$ where l is the axial pole length and r is the armature radius. Then the total flux per increment is:

$$d\phi = B\ l\ r\ d\theta \tag{6}$$

and the total flux per pole is:

$$\phi = \int_a^b B\ l\ r\ d\theta \tag{7}$$

where a and b are the angular limits of a pole.

Substituting equation (5) in (7):

$$\phi = \int_a^b \left\{ B_{max} \left(1 - \frac{k}{2} + \frac{k}{2} \cos 37\theta \right) \right\} l\ r\ d\theta \tag{8}$$

Since:

$$B_{max} = \frac{e}{l\ v} \tag{3}$$

and:

$$v = 2\ \pi\ r\ n \tag{9}$$

where n is rotative speed of armature,

by substitution of (9) and (3) in (8):

$$\phi = \frac{e}{2\ \pi\ n} \int_a^b \left(1 - \frac{k}{2} + \frac{k}{2} \cos 37\theta \right) d\theta \tag{10}$$

or:

$$\phi = \frac{e}{2\ \pi\ n} \left\{ \left(1 - \frac{k}{2} \right) \theta \Big]_a^b + \frac{k}{2(37)} \sin 37\theta \Big]_a^b \right\} \tag{11}$$

where ϕ is in webers if e is in volts and n is in rps.

Let:

$$K_1 = \frac{e}{2\ \pi\ n} \tag{12}$$

$$K_2 = \left(1 - \frac{k}{2} \right) \theta \Big]_a^b \tag{13}$$

$$K_3 = \frac{k}{74} \tag{14}$$

therefore:

$$\phi = K_1 \left\{ K_2 + K_3 \left(\sin 37b - \sin 37a \right) \right\} \tag{15}$$

Sample Calculation: Consider the case when the armature is displaced 0.0104 inches towards pole number 2 under no load conditions; $n = 35$ rps:

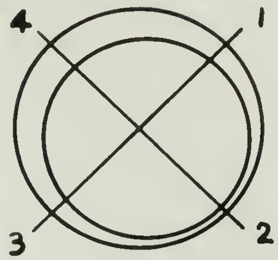

Pole	Air Gap - in	e - volts	K_1
1	0.0625	1.261288×10^{-3}	5.735421×10^{-3}
2	0.0521	1.459248	6.635599
3	0.0625	1.261288	5.735421
4	0.0729	1.204728	5.478227

Pole	k	a radians	b radians	K_2	K_3
1	0.56	0.00000	1.15192	0.8293824	7.567567×10^{-3}
2	0.62	1.57080	2.72272	0.7948248	8.378378
3	0.56	3.14160	4.29352	0.8293824	7.567567
4	0.50	4.71240	5.86432	0.8639400	6.756756

1st Position of Angular Displacement

Pole no. 1

$a = 0^{\circ}$

$b = 66^{\circ}$

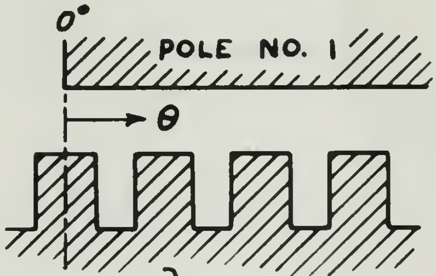

$$\phi_1 = K_1 \left\{ K_2 + K_3 \left[\sin 37b - \sin 37a \right] \right\} \tag{15}$$

$$= K_1 \left\{ K_2 + K_3 \left[\sin 37(66^{\circ}) - \sin 37(0^{\circ}) \right] \right\}$$

$$= K_1 \left\{ K_2 + 7.567567 \times 10^{-3} \left[-0.97815 \right] \right\}$$

$$= K_1 \left\{ 0.8293824 - 0.0074022 \right\}$$

$$= 5.735421 \times 10^{-3} \left\{ 0.8219802 \right\}$$

$\phi_1 = 4.7144025 \times 10^{-3}$ webers

$(\phi_1)^2 = 22.225591 \times 10^{-6}$ $(\text{webers})^2$

In a similar fashion the square of the total flux per pole was determined for poles nos. 2, 3, and 4:

$(\phi_2)^2 = 27.353967 \times 10^{-6}$

$(\phi_3)^2 = 23.033396 \times 10^{-6}$

$(\phi_4)^2 = 22.678349 \times 10^{-6}$

The force on one pole is:

$$f = \frac{1}{2} \frac{\phi^2}{\mu A} \tag{2}$$

f is in newtons when ϕ^2 is in $(\text{webers})^2$,

$\mu = 4\pi \times 10^{-7}$ webers/amp-turn-meter,

and A is pole area in $(\text{meters})^2$.

The constant $\dfrac{1}{2\mu A} = 28.9768 \times 10^6$.

Accordingly the resultant force per pair of opposite poles is:

$$f_{24} = \frac{1}{2\mu A} \left[(\phi_2)^2 - (\phi_4)^2 \right] \tag{16}$$

$$= \frac{1}{2\mu A} \left[27.353967 \times 10^{-6} - 22.678349 \times 10^{-6} \right]$$

$$= 28.9768 \times 10^6 \left[4.675618 \times 10^{-6} \right]$$

$$= 135.48445 \text{ newtons}$$

$$= 30.48400 \text{ pounds}$$

For the remaining pair of poles:

$$f_{31} = \frac{1}{2\mu A} \left[(\phi_3)^2 - (\phi_1)^2 \right] \tag{17}$$

from a similar procedure to that immedietely above:

$f_{31} = 5.26671$ pounds

These forces were resolved into the sum of their vertical components:

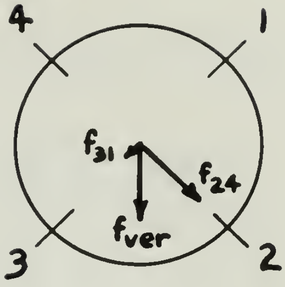

$$f_{ver} = \frac{f_{31} + f_{24}}{2} = 25.2834 \text{ pounds (downwards)} \qquad (18)$$

The latter is the vertical force applied instantaneously for one specific position of angular displacement of the armature. The instantaneous vertical forces were computed for two additional positions of angular displacement:

2nd Position of Angular Displacement - armature rotated 3°

Note: Values of integration limits a and b change accordingly.

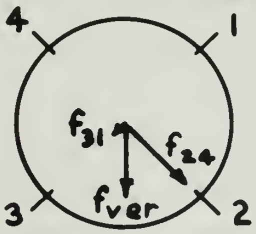

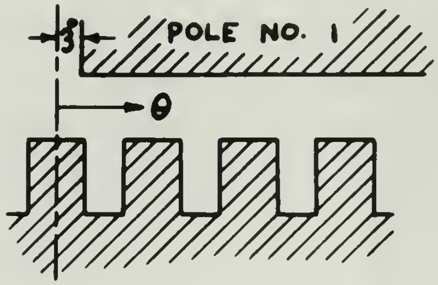

$$f_{ver} = \frac{f_{31} + f_{34}}{2} = 31.6382 \text{ pounds (downwards)} \qquad (18)$$

3rd Position of Angular Displacement - armature rotated 6°

Note: Values of a and b change accordingly.

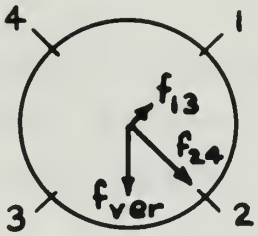

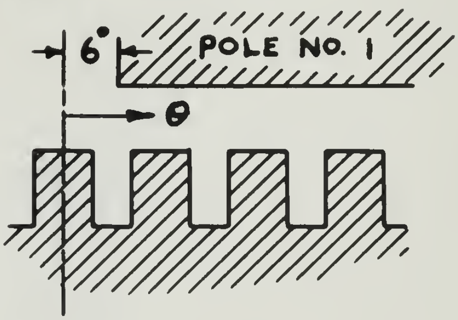

$$f_{ver} = \frac{f_{24} - f_{13}}{2} = 19.9044 \text{ pounds (downwards)} \qquad (19)$$

Presentation of Periodic Force Variation With Angular Position:

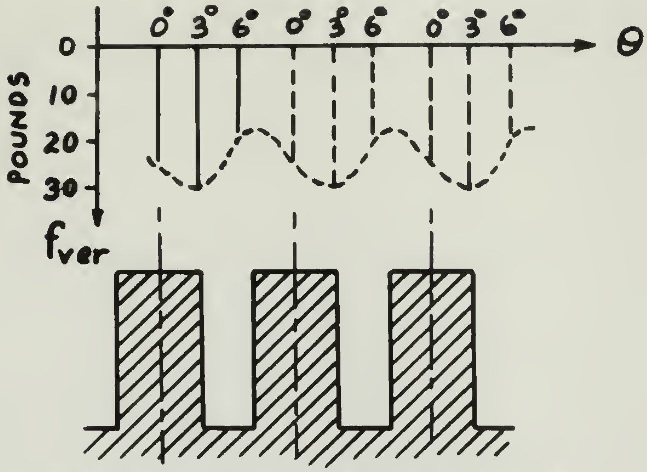

The maximum force variation obtained from the vertical direction is: δf_{ver} = 11.7338 pounds.

Note: The force variation repeats at the same frequency as the number of slots; this may be checked by recalculating for at least one angular position with the integration limits a and b shifted at least one slot pitch, i.e., 0.16981 radians.

The vibration in terms of acceleration is:

$$\text{accel.} = \frac{\delta f_{ver}}{w/g} = 0.797 \text{ ft/sec}^2 \tag{20}$$

where w = 474 pounds (total weight on spring system), and $g = 32.2 \text{ ft/sec}^2$

or: accel. = 24.3 cm/sec^2.

Expressed in decibels with 0.001 cm/sec^2 as a reference:

$$\text{Vibration Level} = 20 \log_{10} \frac{\text{accel.}}{0.001} \tag{21}$$

$$= 20 \log_{10} \frac{24.3}{0.001}$$

$$= 87.7 \text{ decibels}$$

APPENDIX B

DATA

VIBRATION DATA

No-load and load vibration data are contained in Tables I, II, and III. Symbols used are explained below.

Frequency Harmonic

1, 2, 3, etc. refer to first harmonic (fundamental), second harmonic, third harmonic, etc.

F is used to designate motor rotational speed in cycles per second.

S is used to designate armature slot frequency in cycles per second.

B is used to designate the eddy-current brake slot frequency in cycles per second, and equals the product of the number of slots (8) in the eddy-current brake disk and the motor rotational speed in cycles per second.

Over-all designates the over-all noise (vibration) level in decibels.

Over-all (corrected) is the over-all noise level corrected for the effect of the eddy-current brake contribution. This correction appears only in load test tabulation of data.

No-load vibration data used to obtain vibratory forces are contained in Tables I and II.

AIR-GAP FLUX-DENSITY DATA

Figure XIV shows the voltage waveform (and flux-density waveform) existing in the air gap for various armature positions of the no-load test. Figure XV shows the oscilloscope voltage calibration curve used in determining the voltage induced in the wire pickup.

TABLE I

NO-LOAD DATA

Pickup Position : Slip-Ring End, Vertical

Motor Speed : 2100 RPM

NOISE LEVEL IN DECIBELS

Frequency Harmonic	Armature Position Centered	0.0104 (inch) Off-ctr	0.0205 (inch) Off-ctr	0.0300 (inch) Off-ctr	0.0386 (inch) Off-ctr
1F	75	76	76	75	76
2F	73	75	76	76	75
3F	78	76	76	77	78
4F	74	77	78	76	78
5F	81	87	88	88	92
6F	87	90	94	94	98
1S	85	89	92	94	103
2S	90	91	92	93	94
3S	76	83	75	77	78
4S	86	86	87	90	84
5S	88	84	87	88	86
6S	--	--	--	--	--
Over-all	104	104	104	107	109

TABLE II

NO-LOAD DATA

Pickup Position : Slip-Ring End, Vertical

Motor Speed : 2100 RPM

NOISE LEVEL IN DECIBELS

Frequency Harmonic	Armature Position Centered	0.0104 (inch) Off-ctr	0.0205 (inch) Off-ctr	0.0300 (inch) Off-ctr	0.0386 (inch) Off-ctr
1F	75	76	75	76	72
2F	74	74	75	74	72
3F	75	76	73	76	74
4F	70	73	75	77	75
5F	79	87	87	88	87
6F	90	90	92	93	95
1S	83	87	91	94	100
2S	91	93	93	92	90
3S	73	76	76	76	73
4S	84	86	86	86	80
5S	86	88	86	86	84
6S	--	--	--	--	--
Over-all	101	102	104	105	108

TABLE III

LOAD DATA

Pickup Position : Slip-Ring, Vertical

Motor Speed : 2000 RPM

NOISE LEVEL IN DECIBELS

Frequency Harmonic	Centered	Armature Position 0.0104 (inch) Off-ctr	0.0205 (inch) Off-ctr	0.0300 (inch) Off-ctr	0.0386 (inch) Off-ctr
1F	94	93	93	95	95
2F	83	84	83	88	89
3F	85	87	85	90	92
4F	88	89	88	93	93
5F	96	96	94	98	97
6F	98	100	98	101	103
1S	96	98	98	98	105
2S	87	90	90	92	94
3S	78	82	79	85	85
4S	79	86	84	88	87
5S	81	88	88	91	88
6S	78	87	87	84	84
1B	117	119	116	120	121
2B	91	92	92	101	100
3B	98	98	98	102	102
Over-all	118	120	118	124	124
Over-all (corrected)	111	113	114	120	121
Tare Weight Applied (kg)	1.15	1.20	1.15	1.15	1.12
Applied Load (horsepower)	1.125	1.174	1.125	1.125	1.096

Figure XIV

Air Gap Flux Density Distributions

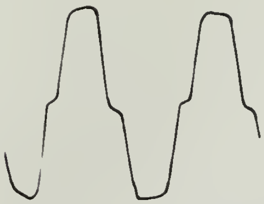

Armature Centered
Total Deflection 24.5 units

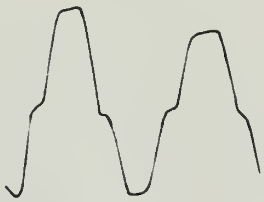

Armature Displaced 0.0104 in.
Total Deflection 24.5 units

Armature Displaced 0.0205 in.
Total Deflection 25.5 units

Armature Displaced 0.0300 in.
Total Deflection 25.5 units

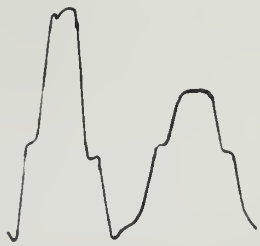

Armature Displaced 0.0386 in.
Total Deflection 30.0 units

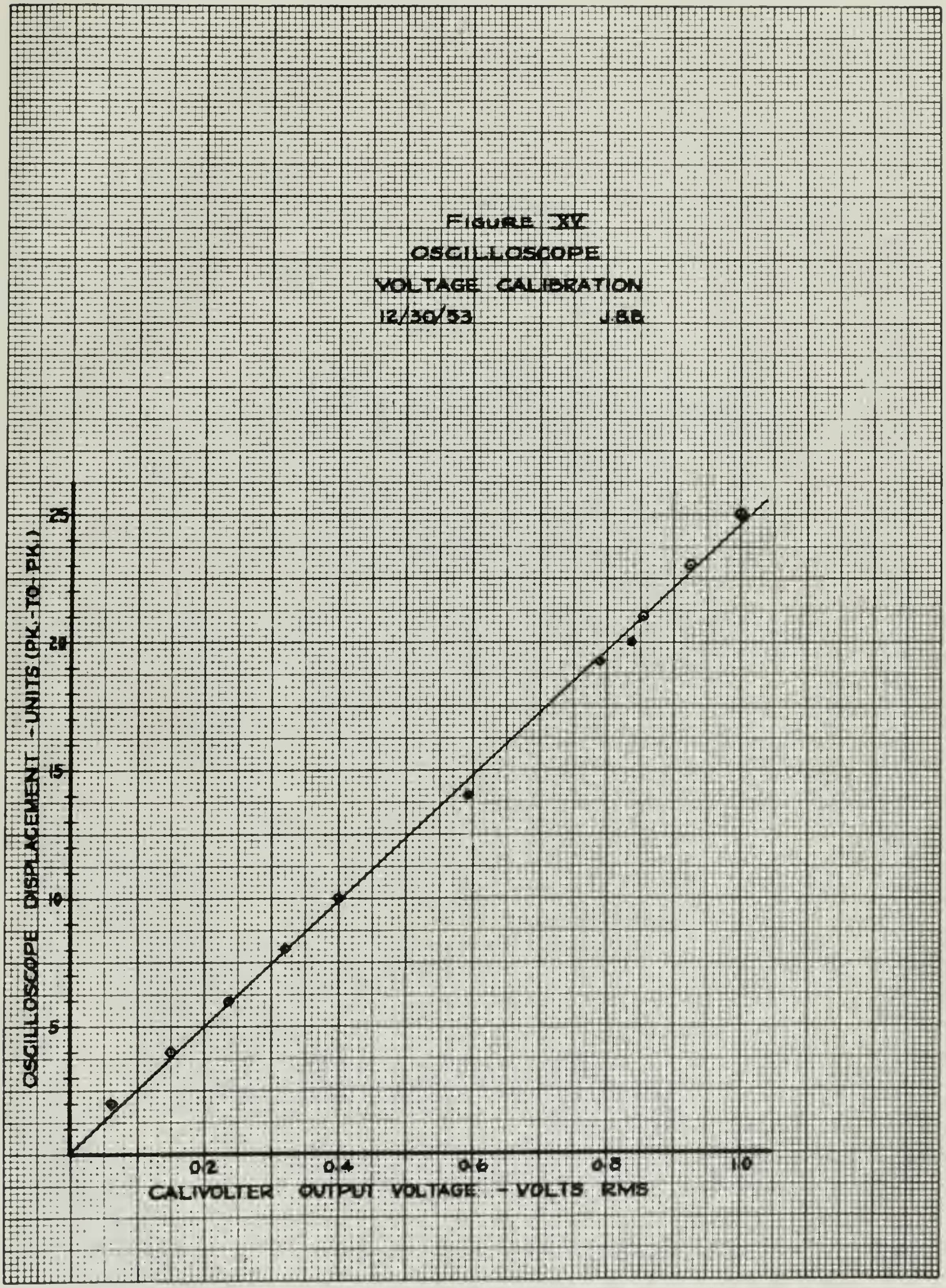
Figure XV
OSCILLOSCOPE
VOLTAGE CALIBRATION
12/30/53
J.B.B.
OSCILLOSCOPE DISPLACEMENT - UNITS (PK.-TO-PK.)
5
10
15
20
25
0.2
0.4
0.6
0.8
1.0
CALIVOLTER OUTPUT VOLTAGE - VOLTS RMS

APPENDIX C

APPENDIX C

MOTOR IDENTIFICATION

The motor selected for study is characteristic of the type and size used for submarine auxiliary machinery of World War II vintage. It is identifiable by the following:

D-324 drip-proof semi-enclosed self-vent motor; 7 1/2 H.P.; direct-current; shunt stabilized windings; 1800 to 2250 RPM; 26 amperes F.L.; 250 volts; manufactured by Electro Dynamic Works of the Electric Boat Company, Bayonne, New Jersey; manufacturer's Plan No. D-36463; Navy Department, Bureau of Ships Plan No. SS212-563-09.

APPENDIX D

APPENDIX D

LITERATURE CITATIONS

1 Alger, John R.M., "Some Effects of Eccentric Air Gap in Induction Machines," MIT E.E. Thesis, 1950.

2 Alger, P.L. and Kennelly, A.E., "Magnetic Flux Distribution in Annular Steel Laminae," MIT Research Division Bulletin No. 16.

3 Allen, J.E., Ballantyne, W.M.H., and Baudry, R.A., "Investigation and Elimination of Unusual Vibration in the Field on a Large Single-Phase Frequency Changer," AIEE Transactions, 69, 1950, p. 1264.

4 Appleman, W.R., "The Cause and Elimination of Noise in Small Motors," AIEE Transactions, 56, 1937, p. 1369.

5 Electrical Engineering Staff, MIT, Magnetic Circuits and Transformers (John Wiley and Sons, New York) 1943.

6 Eldred, K.M., Francis, J.J., and Gold, P.D., "A Resume of the Application of Vibration Engineering to the Solution of Marine Operational Problems Encountered by Naval Vessels," New England Section of the Society of Naval Architects and Marine Engineers, January, 1953.

7 Fitzgerald, A.E. and Kingsley, C., Jr., Electric Machinery (McGraw-Hill, New York) 1949.

8 Goldman, S., Frequency Analysis, Modulation and Noise (McGraw-Hill, New York) 1948.

9 Green, C.H. and Johnson, E.E., "Graphical Determination of Magnetic Fields, Comparison of Calculations, and Tests," AIEE Transactions, 46, 1927, p. 136.

10 Greenwood, L., Design of D-C Machines (MacDonal and Co., Ltd., London) 1949.

11 MacMillan, F. and Staples, D.R., "Investigation of Induction Motor Noise," MIT E.E. Thesis, 1925.

LITERATURE CITATIONS (continued)

12 Morrill, W.J., "Harmonic Theory of Noise in Induction Motors," AIEE Transactions, 59, 1940, p. 474.

13 Morse, P.M., Vibration and Sound (McGraw-Hill, New York) 1936.

14 Park, R.H. and Stevenson, A.R., "Graphical Determination of Magnetic Fields, Theoretical Considerations," AIEE Transactions, 46, 1927, p. 112.

15 Wieseman, R.W., "Graphical Determination of Magnetic Fields, Practical Applications to Salient-Pole Synchronous Machine Design," AIEE Transactions, 46, 1927, p. 141.